Title
INITIAL SINTERING OF Al203 POWDER COMPACTS BY HOT STAGE SCANNING ELECTRON MICROSCOPY

Author
Wang, D.N.K.

Publication Date
1977-05-01

Submitted to American Ceramic Society

LBL-6239
Preprint c. 2

INITIAL SINTERING OF Al_2O_3 POWDER COMPACTS BY HOT STAGE SCANNING ELECTRON MICROSCOPY

D. N. K. Wang and R. M. Fulrath

May 1977

Prepared for the U. S. Energy Research and Development Administration under Contract W-7405-ENG-48

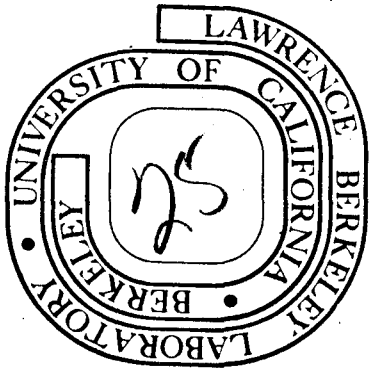

DISCLAIMER

INITIAL SINTERING OF Al_2O_3 POWDER COMPACTS BY HOT STAGE SCANNING ELECTRON MICROSCOPY

D. N. K. Wang and R. M. Fulrath

Materials and Molecular Research Division, Lawrence Berkeley Laboratory
and Department of Materials Science and Mineral Engineering,
University of California, Berkeley, California 94720

ABSTRACT

Initial stage sintering of different types of MgO-doped Al_2O_3 powders was studied by measuring powder compact densification at various constant rates of heating. Hot stage scanning electron microscopy was used to monitor continuously the linear dimensional change of the powder compact during sintering. Using a theoretical model for the initial stage as an interpretative tool in the analysis of sintering data, it has been found that "non-reactive" A-14 Al_2O_3 powder sintered with a higher activation energy than "reactive" submicron Al_2O_3 powders.

INTRODUCTION

Isothermal studies of linear dimensional changes of powder compacts have provided most of the available sintering data on the initial stage process. Isothermal experiments present several problems, of which the most important is the inability to study adequately the initial portion of the sintering process, because the most rapid shrinkage occurs while thermal equilibrium is still being established.

To circumvent this problem, sintering has been studied by measuring densification using a constant rate of heating (CRH) technique. In particular, Young and Cutler[1] have studied elutriated Alcoa A-14 alumina powders. Because only one heating rate was used in their work, the true activation energy for sintering was not obtained. In studying UO_2 powders and ThO_2 gels, Woolfrey and Bannister[2] obtained the sintering rate law by performing CRH experiments at different heating rates. By comparing results from isothermal experiments performed on the same material, they have claimed that they demonstrated the validity and accuracy of the nonisothermal technique.

Alcoa A-14 Al_2O_3 powder is generally described as "dead burned" or "non-reactive" material, while submicron size Al_2O_3 powders prepared by heating decomposable salts are generally described as "reactive" materials. It was the main purpose of this work to compare the initial stage sintering behavior of these powders. In addition, a study of sintering behavior with variations in green compact density was also made. Hot stage scanning electron microscopy was used to monitor the linear dimensional change of a powder compact at various constant heating rates. This technique has several advantages when compared with

other methods: (1) It provides a means to monitor continuously the dimensional changes of a specimen during the sintering process. (2) The temperature gradient across the specimen is negligible during heating because of the small size of the specimen. (3) It makes possible a statistical analysis of the sintering results.

It is generally accepted that the theoretical models derived from idealized geometries may not truly describe the sintering kinetics of a real powder compact. This is due to the fact that a real powder compact normally consists of a random distribution of particles varying in shape, size, packing geometry and surface geometry. Nevertheless, the theoretical models have proved to be valuable as an interpretative tool in the analysis of sintering data[3] and will be used in the present work to study the difference in the sintering behavior of different types of Al_2O_3 powders.

Following Bannister,[4] the differential form of the initial stage sintering equation is

$$\frac{d\left(\frac{\Delta L}{L_o}\right)}{dt} = \frac{K}{\left(\frac{\Delta L}{L_o}\right)^{n-1}} \tag{1}$$

where constants K and n depend on the geometry and the material transport mechanism, $\frac{\Delta L}{L_o}$ is the fractional shrinkage, and t is the time. For the sintering of spherical particles, when the rate controlling mechanism is volume diffusion:

$$K = (1.95\gamma\Omega D_v / r^3 kT) \text{ and } n=2.0 \tag{2}$$

For grain-boundary diffusion:

$$K = (0.48\gamma b\Omega b D_b / r^4 kT) \text{ and } n=3.1 \tag{3}$$

where γ is the surface energy, Ω is the volume of a vacancy, D_b is the grain-boundary diffusion coefficient, b is the effective grain-boundary width , D_v is the volume diffusion coefficient, k the Boltzmann constant, r is the particle radius, and T is the absolute temperature. The temperature dependence of K can be represented by

$$K = K_o \exp\left(-\frac{Q}{RT}\right) \tag{4}$$

where K_o is proportional to $\frac{1}{T}$. The equation, which applies to CRH conditions, is obtained from equation (1) and (4):

$$\frac{d\left(\frac{\Delta L}{L_o}\right)}{dt} = \frac{\left[K_o \exp\left(-\frac{Q}{RT}\right)\right]}{\left(\frac{\Delta L}{L_o}\right)^{n-1}} \tag{5}$$

This equation is based on the assumption that, at any state of shrinkage and temperature, the isothermal and onisothermal shrinkage rates are equal. After substitution of the constant heating rate, $a = \frac{dT}{dt}$, and rearrangement, equation (5) becomes:

$$a\left(\frac{\Delta L}{L_o}\right)^{n-1} d\left(\frac{\Delta L}{L_o}\right) \Big/ dT = K_o \exp\left(-\frac{Q}{RT}\right) \tag{6}$$

If Q and n, which are characteristic of the rate controlling mechanism remain constant and θ is the temperature:

$$\left(\frac{\Delta L}{L_o}\right)^n = \left(\frac{n}{a}\right)\int_o^T K_o \exp\left(-\frac{Q}{R\theta}\right)^{d\theta} \tag{7}$$

Since Q>>RT equation (7) may be approximated by

$$\left(\frac{\Delta L}{L_o}\right)^n = \left[K_o R T^2 \left(\frac{n}{aQ}\right)\right] \exp\left(-\frac{Q}{RT}\right) \tag{8}$$

Elimination of $\frac{\Delta L}{L_o}$ from equation (6) and (8) provides the shrinkage rate equation:

$$\frac{d\left(\frac{\Delta L}{L_o}\right)}{dt} = \left(K_o\right)^{\frac{1}{n}} \left[\frac{aQ}{RT^2 n}\right]^{\frac{n-1}{n}} \exp\left(-\frac{Q}{nRT}\right) \tag{9}$$

Substituting equations (4) and (5) into (9) provides the following equation:

$$T^2 \frac{d\left(\frac{\Delta L}{L_o}\right)}{dt} \Big/ a = \left(\frac{Q}{nR}\right)\left(\frac{\Delta L}{L_o}\right) \tag{10}$$

Thus a linear-linear plot of $T^2 \frac{d\left(\frac{\Delta L}{L_o}\right)}{dt} \Big/ a$ vs. $\frac{\Delta L}{L_o}$ should give a straight line with slope $\frac{Q}{nR}$. From this slope, the effective activation energy, $\frac{Q}{n}$ can be determined. From equation (8), a ℓn-ℓn plot of fractional shrinkage at a specific temperature vs. heating rate gives a straight line of slope of $-\frac{1}{n}$. Therefore, the apparent activation energy, Q, can be determined. Another way to obtain the value of $\frac{Q}{nR}$ is from the simplified plot of the form $\ell n \frac{\Delta L}{L_o T}$ vs. $\frac{1}{T}$. This type of plot has been used by Young and Cutler[1] to determine the effective activation energy. In a real situation, transient shrinkage, caused either by the formation of new contacts between the particles or by particle sliding, will be included in the total shrinkage. This error can be minimized if the equation involving the derivative of shrinkage is used. Therefore, in the present work, a differential plot of shrinkage is preferred in determining the sintering kinetics.

EXPERIMENTAL PROCEDURE

Four different types of aluminum oxide powders were used. They were Alcoa A-14 Al_2O_3 and three submicron size powders prepared by heating decomposable salts from different sources.* The compacts were made by cold pressing the powders, to which 0.1 wt% of MgO and appropriate organic binder (PVA) were added. The amount of binder added depended on the surface area of the powders. The greater the surface area of the powders the larger the amount of binder needed. It ranged from 1 wt% to 8 wt%. All the cold pressed specimens had a diameter of 0.2 inch and a thickness of 0.1 inch. Alcoa A-14 Al_2O_3 powder was wet ground for 16 hours in a high purity (99.98%) alumina lined rotating mill, dried and pressed. This procedure was used to break up agglomerates. The powder had an average particle size of 2.5μm. The size of the submicron Al_2O_3 powders were determined by scanning electron microscopy to be 0.1μm for the Grace powder, 0.2μm for the General Electric powder and 0.3μm for the Union Carbide powder. The Alcoa A-14 powder particles were prismatic in shape and the submicron powders were more cylindrical in shape with no crystallographic morphology. These compacts were prefired at 650°C in air for one hour to decompose the organic binder. The green densities of the specimens were determined after the prefiring.

---

*Union Carbide Linde-A alumina (Lot No. 1006). W. R. Grace & Co. high purity alumina (Lot No. 2156A-52). General Electric Company Autoclaved high purity alumina.

To study the linear dimensional change of the specimen during experiments, tungsten microspheres were placed on the specimen surface to serve as referrence points. The compacts were then heated in the hot stage of the scanning electron microscope under programmed heating rates, ranging from 1°C to 13°C/min. The vacuum in the hot stage chamber was about 3×10^{-5} torr. During each sintering run, a 16mm movie was made of the TV screen and recorded continuously the movement of the tungsten markers. Linear dimensional changes were made by measuring the distance, an average distance of 1,000 to 10,000 particle diameters, between specific microspheres. At least eight measurements at different directions on the sample surface provide an average shrinkage for each temperature. Since the fractional shrinkage $\frac{L_o - L}{L_o}$ at all temperatures were determined with the same low temperature value of L_o, a thermal expansion correction[6] was made for each of the measurements. A detailed description of the principles of this technique has been reported elsewhere.[7]

RESULTS AND DISCUSSION

The fractional shrinkage vs. temperature plots for two of the four powders during sintering are presented in Figs. 1 and 2. Figure 3 gives the results for all the aluminum oxide powders which were plotted according to equation (10). Two different slopes for each powder are noted. Equation (10) indicates that the plot should exhibit a single slope if (1) the material contains particles of a single size and (2) a single diffusion mechanism operates or if a combination of mechanisms with the same activation energy predominates over the entire initial stage.

The problem of multiple mechanisms in sintering kinetics was treated by Johnson.[8] He has observed that low activation energy surface diffusion, acting in consort with grain-boundary diffusion, results in an abnormally high apparent activation energy for densification. This situation has been described in detail by Cutler[1]. Surface diffusion generally has a low activation energy, and it is expected to be the predominant mass transport mechanism at temperatures at or below the initial shrinkage temperature. If a neck is formed by surface diffused material, the flow of material from the grain-boundary, which is normally to the neck, is impeded until a temperature is reached at which flow from the grain-boundary predominates. The net effect is a steepened initial slope. The independence of the slopes obtained in Fig. 3 with the heating rate for the submicron powders indicates that surface diffusion as a competing mechanism is unlikely. The other mechanism that might be confused with surface diffusion is the volume-to-grain boundary changeover proposed by Johnson and Berrin[9]. These alternatives are difficult to distinguish.

The most significant thing found in this experiment is that the effective activation energies calculated from the slopes are different for A-14 Al_2O_3 powder and the submicron size Al_2O_3 powders. The effective activation energy, $\frac{Q}{n}$, for A-14 powder is 75 Kcal/mole below 2.2% fractional shrinkage and 42 Kcal/mole above 2.2%. These results give fairly good agreement with the effective activation energies of 83±10 and 38±3 Kcal/mole, respectively, obtained by Young and Cutler[1] who used an Arrhenius - type plot. The two effective activation energies calculated for the submicron size powders are 44 and 30 Kcal/mole with the break point at approximately 2% fractional shrinkage. Green density did not affect the sintering law or the effective activation energy as seen in Fig. 3. A decrease in green density for Union Carbide powder compact, from 38 to 32% theoretical density, only led to progressively reduced rates of sintering. This phenomenon was also observed by Woolfrey with UO_2 material.[10]

Data obtained from Figs. 1 and 2 are plotted in Figs. 4 and 5 respectively, as ℓn shrinkage at a given temperature vs. ℓn heating rate. In these plots, the values of n calculated from the slopes indicate that n increases from ~1.5 and levels off at a value of 3. The dashed lines drawn in these figures represent the transitions between $n \neq 3$ and $n = 3$. This same result was also observed for the other two powders. The transitions between regions are not as apparent as the break points in slopes as seen in Fig. 3. However, they are consistent with the observed variations in effective activation energies over these ranges of temperature and shrinkage.

Because of the ambiguous nature of the lower portions of the kinetics in Fig. 3, further analysis will concentrate on the upper regions of the curves.

The value of n ($\approx$3) observed for the upper portions of the curves is that expected for grain boundary-diffusion and indicates that this is probably the rate-controlling mechanism. The parameters γ and Ω in equation (3) were assigned the values 1,000 ergs/cm^2 and 10^{-23} cm^3, respectively. The particle sizes, r, were 0.1, 0.2, 0.3 and 2.5 microns for the W. R. Grace, General Electric, Union Carbide and Alcoa A-14 Al_2O_3 powders, respectively. The diffusion coefficients, calculated by using equations (1) and (3), are shown in Fig. 6. Diffusion coefficients given by other sources[11-15] are also shown. The bD_b and D_v values are given on the same plot although they are not directly comparable. The discrepancy in the bD_b value calculated for Union Carbide powder from that of the other two submicron size powders may arise from difficulties in determining the actual particle size and/or from the differences in grain-boundary width. The activation energy for the diffusion process obtained for all these submicron size powders has the same value of 93 Kcal/mole. This agrees very well with the value of 90 Kcal/mole that was observed by Chang[14] in his deformation experiments. However, the activation energy calculated for A-14 Al_2O_3 is 142 Kcal/mole assuming grain-boundary diffusion. This could be attributed to the lack of validity of equation (3) when applied to A-14 Al_2O_3 powder. In fact, the particle shape of A-14 alumina strongly deviates from the spherical shape assumed in using equation (3).

In studying the shape sensitivity of initial sintering, Bannister[4] found that n may be affected as much by the contact geometry as by the material transport mechanism. Depending on the geometry, a value of n = 3 may indicate either volume or grain-boundary diffusion. For the pyramid-pyramid and pyramid-plate geometries, a value of n = 3 indicates that the rate controlling mechanism is volume diffusion. The factor K used in equation (1) is the same as that in equation (2) except that the numerical value changes with changing apex angle. Using 11.4 as the numerical value[4] in equation (2), the calculated volume diffusion coefficients for A-14 Al_2O_3 is plotted in Fig. 6. These results give an activation energy of 150 Kcal/mole which is approximately the same as previous values[12,15] obtained by assuming a volume diffusion mechanism.

CONCLUSIONS

Hot stage scanning electron microscopy has proven to be useful for the study of the sintering process. This work has provided the first experimental results on the initial stage sintering of MgO-doped Al_2O_3 powder compacts in a vacuum environment. With the absence of further evidence, it appears that in the initial stage sintering a grain-boundary diffusion mechanism is responsible for mass transport in submicron size Al_2O_3 powders and a volume diffusion mechanism is responsible in Alcoa A-14 Al_2O_3 powder.

ACKNOWLEDGEMENT

This work was supported by the U.S. Energy Research and Development Administration.

REFERENCES

1. W. S. Young and I. B. Cutler, "Initial Sintering with Constant Rates of Heating," J. Am. Cer. Soc., Vol. 53 [12], 659-663 (1970).

2. J. L. Woolfrey and M. J. Bannister, "Nonisothermal Techniques for Studying Initial - Stage Sintering," J. Am. Cer. Soc.,Vol. 55 [8], 390-394 (1972).

3. M. Astier, and P. Vergnon, "Determination of the Diffusion Coefficients from Sintering Data of Ultrafine Oxide Particles," J. Solid State Chemistry 19, 67-73 (1976).

4. M. J. Bannister, "Shape Sensitivity of Initial Sintering Equations," J. Am. Cer. Soc., Vol. 51 [10], 548-553 (1968).

5. S. Young, S. Rasmussen and I. B. Cutler; pp. 185-202 in Ultrafine - Grain Ceramics. Edited by J. J. Burke, N. L. Reed, and Volker Weiss. Syracuse University Press, Syracuse, NY (1970).

6. T. H. Nielsen and M. H. Leipold, "Thermal Expansion in Air of Ceramic Oxides to 2200°C," J. Am. Cer. Soc., 46 [8] 381-387 (1963).

7. D. N. K. Wang, "Sintering of Al_2O_3 Powder Compact by Hot Stage Scanning Electron Microscopy"; Ph.D. Thesis, University of California, Berkeley, 1976.

8. D. L. Johnson, "Interpretation of Sintering Kinetics Data," in "Sintering and Related Phenomena". Edited by G. C. Kuczynski, Materials Sc. Res. [6], 363-368, Plenum Press, NY (1973).

9. D. L. Johnson and L. Berrin; pp. 445-69 in "Sintering and Related Phenomena". Edited by G. C. Kuczynski, N. A. Hooton, and C. F. Gibbon. Gordon & Breach Science Publishers, Inc., NY (1967).

10. J. L. Woolfrey, "Effect of Green Density on the Initial-Stage Sintering Kinetics of UO_2," J. Am. Cer. Soc., Vol. 55 [8], 383-389 (1972).

11. A. E. Paladino and W. D. Kingery, "Aluminum Ion Diffusion in Aluminum Oxide," J. Chem. Phys., 37 [5] 957-62 (1962).

12. R. L. Coble, "Initial Sintering of Alumina and Hematite," J. Am. Cer. Soc., Vol. 41 [2] (1958).

13. Y. Oishi and W. D. Kingery, "Self-Diffusion of Oxygen in Single Crystal and Polycrystalline Aluminum Oxide," J. Chem. Phys. 33 [2] 480-86 (1960).

14. C. Chang, "Diffusion-Controlled Deformation and Shape Changes in Nonfissionable Ceramics," Proceeding of the Conference on "Nuclear Applications of Nonfissionable Ceramics," pp. 101-112, edited by Alvin Boltax and J. H. Handwerk, Washington, DC (1966).

15. R. L. Coble, "Sintering Crystalline Solids: II. Experimental Test of Diffusion Models in Powder Compacts," J. Appl. Phys., 32 [5] 793-99 (1961).

FIGURE CAPTIONS

1. Densification profiles of Alcoa A-14 Al_2O_3 powder compacts at various constant heating rates.
2. Densification profiles of W. R. Grace Al_2O_3 powder compacts as various constant heating rates.
3. Plot of $T^2[d(\Delta L/L_o)/dt]/a$ vs. $(\Delta L/L_o)$ for initial stage sintering of four different types of 0.1 wt% MgO-doped Al_2O_3 powder compacts with various constant heating rates.
4. Effect of heating rate on shrinkage at a specific temperature for initial stage CRH sintering of Alcoa A-14 Al_2O_3 powder compact.
5. Effect of heating rate on shrinkage at a specific temperature for initial stage CRH sintering of W. R. Grace Al_2O_3 powder compact.
6. Diffusion coefficients calculated from initial stage sintering data compared with directly measured (tracer) values in Al_2O_3. (a) Ref. 11, (b) Ref. 15, (c) Ref. 12, (d) (e) Ref. 13 and (f) Ref. 14.

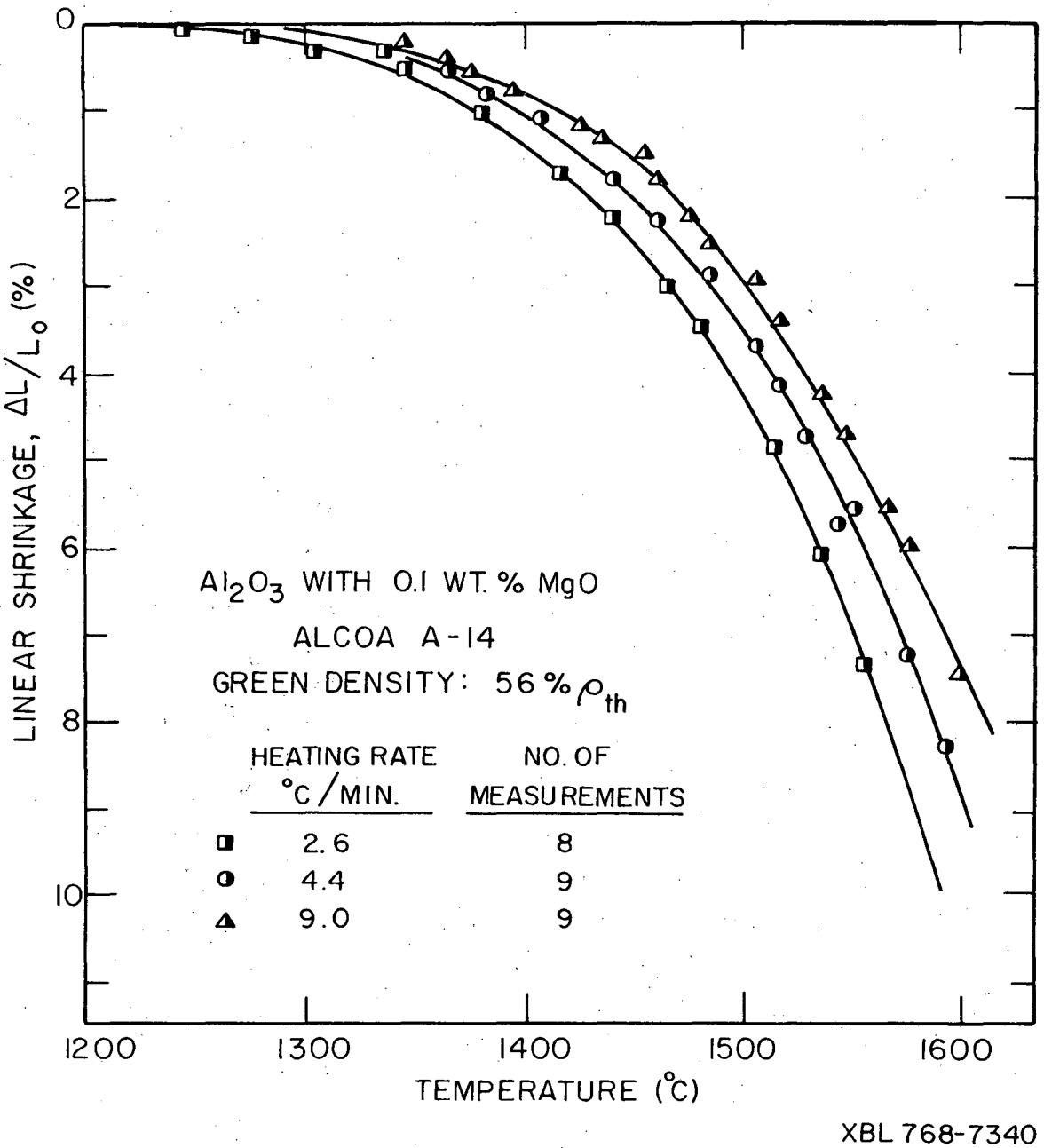
LINEAR SHRINKAGE, $\Delta L/L_o$ (%)
0
2
4
6
8
10
1200
1300
1400
1500
1600
TEMPERATURE (°C)
Al_2O_3 WITH 0.1 WT. % MgO
ALCOA A-14
GREEN DENSITY: 56 % ρ_{th}
HEATING RATE °C/MIN.
NO. OF MEASUREMENTS
2.6
8
4.4
9
9.0
9
XBL 768-7340

Figure 1.

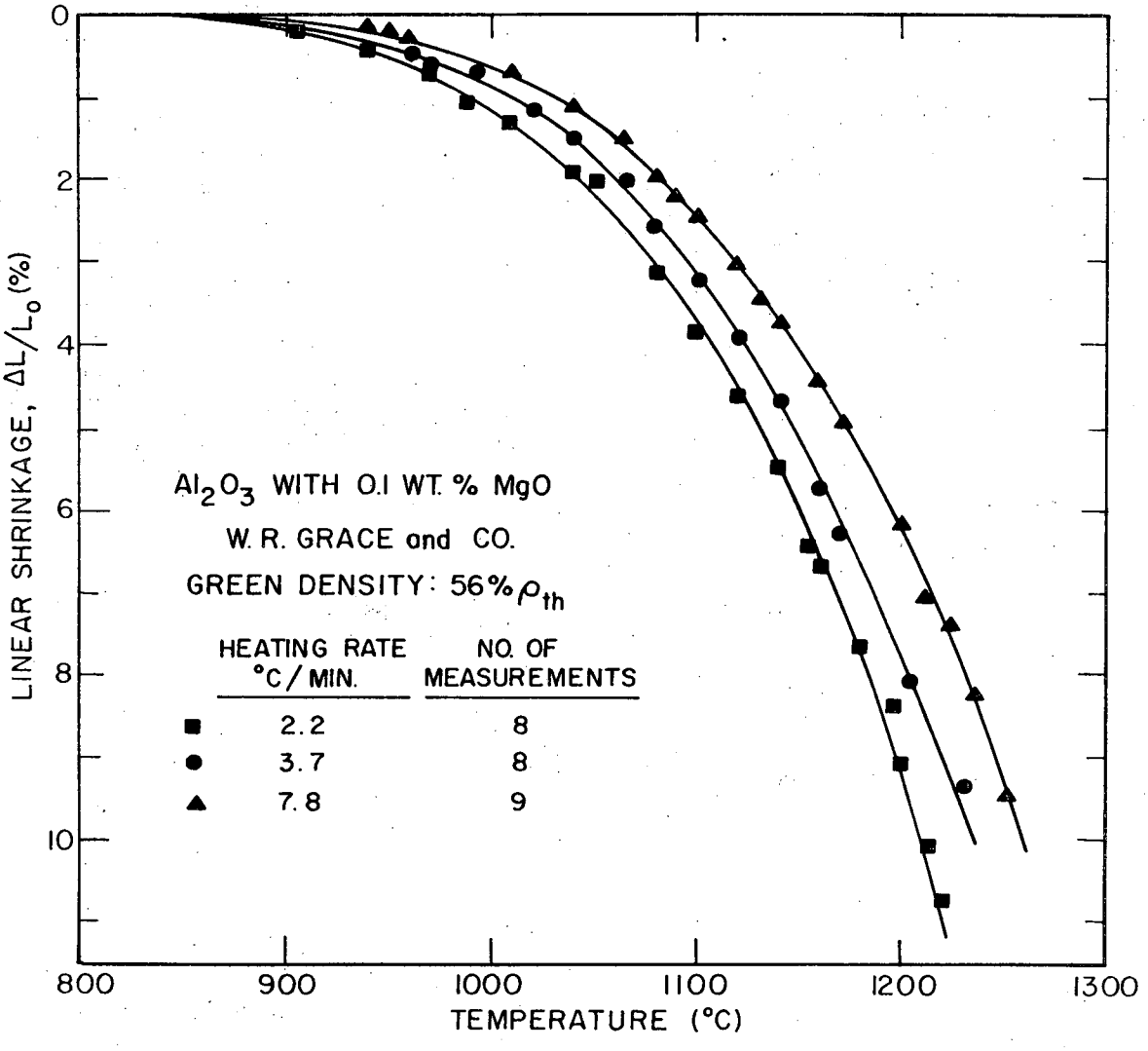
LINEAR SHRINKAGE, $\Delta L/L_o$ (%)
0
2
4
6
8
10
800
900
1000
1100
1200
1300
TEMPERATURE (°C)
Al_2O_3 WITH 0.1 WT. % MgO
W. R. GRACE and CO.
GREEN DENSITY: 56% ρ_{th}
HEATING RATE °C / MIN.
NO. OF MEASUREMENTS
2.2
8
3.7
8
7.8
9
XBL 768-7339

Figure 2.

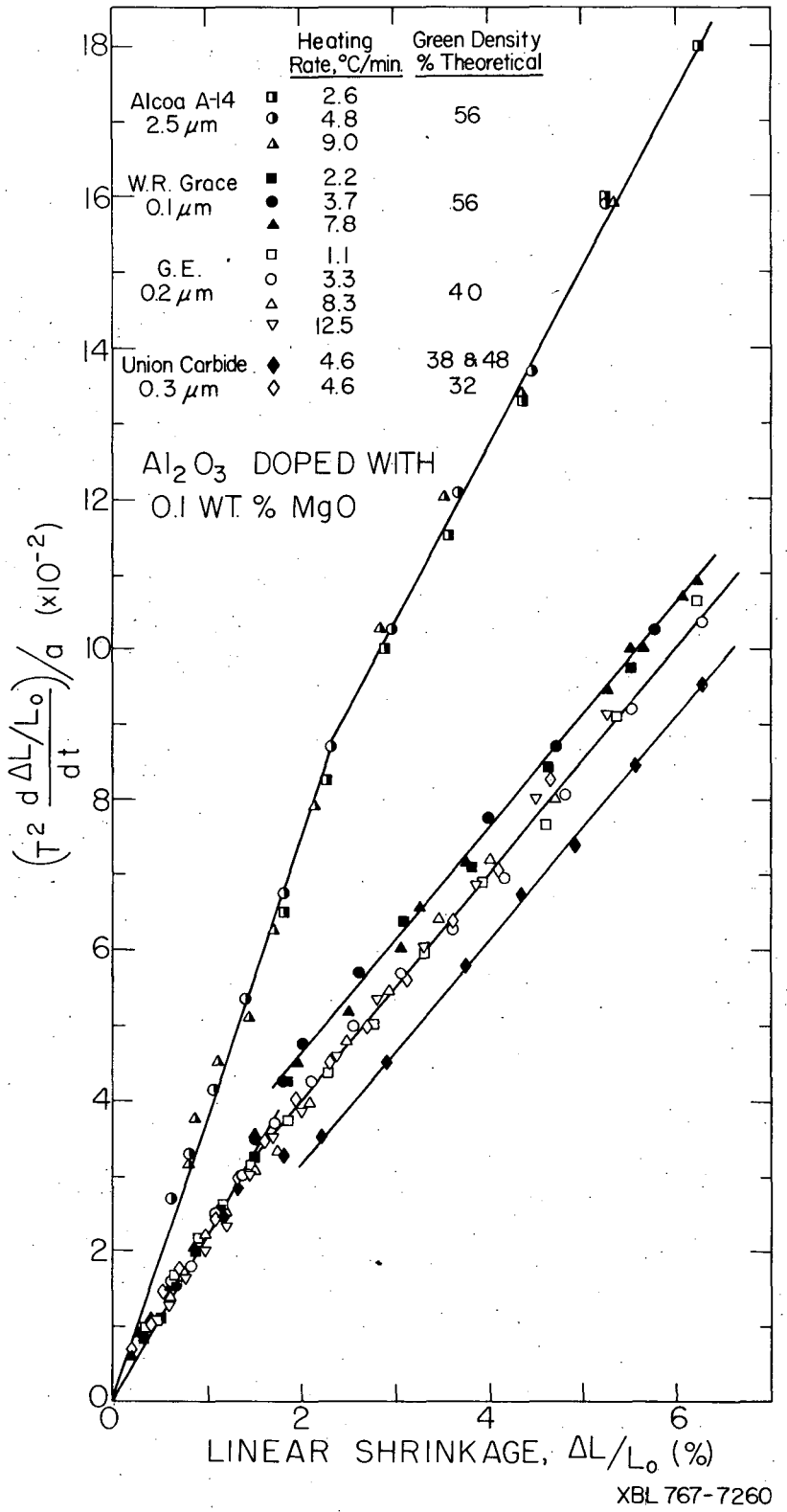
Heating Rate, °C/min.
Green Density % Theoretical
Alcoa A-14 2.5 μm
2.6
4.8
9.0
56
W.R. Grace 0.1 μm
2.2
3.7
7.8
56
G.E. 0.2 μm
1.1
3.3
8.3
12.5
40
Union Carbide 0.3 μm
4.6
4.6
38 & 48
32
Al2O3 DOPED WITH 0.1 WT. % MgO
$\left(T^2 \frac{d\,\Delta L/L_o}{dt}\right)/a$ (x10^{-2})
LINEAR SHRINKAGE, $\Delta L/L_o$ (%)
0
2
4
6
8
10
12
14
16
18
XBL 767-7260

Figure 3.

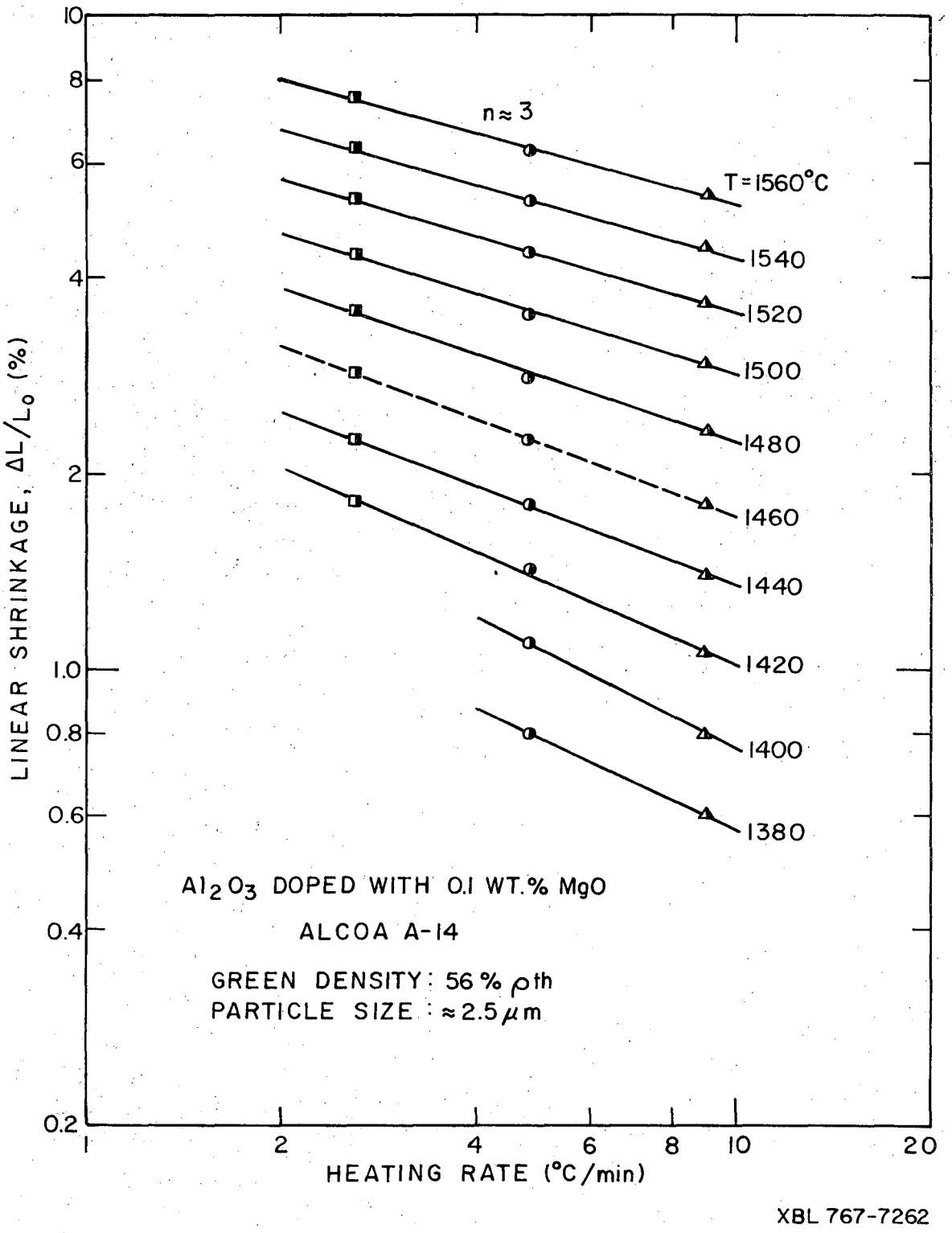
LINEAR SHRINKAGE, $\Delta L/L_o$ (%)
HEATING RATE (°C/min)
n ≈ 3
T = 1560°C
1540
1520
1500
1480
1460
1440
1420
1400
1380
Al_2O_3 DOPED WITH 0.1 WT.% MgO
ALCOA A-14
GREEN DENSITY: 56 % ρth
PARTICLE SIZE : ≈2.5 μm
XBL 767-7262

Figure 4.

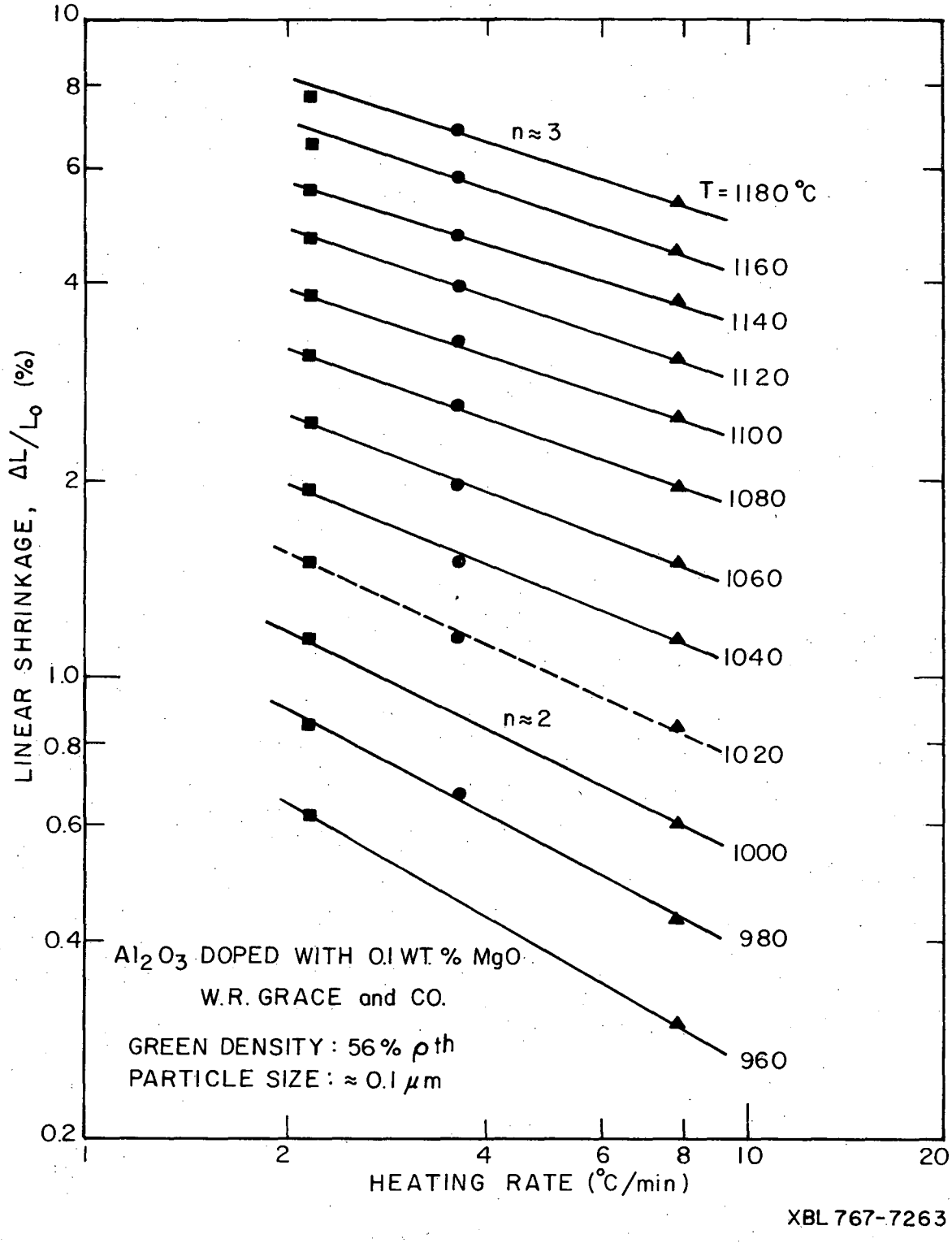
LINEAR SHRINKAGE, $\Delta L/L_o$ (%)
HEATING RATE (°C/min)
n≈3
n≈2
T=1180°C
1160
1140
1120
1100
1080
1060
1040
1020
1000
980
960
Al_2O_3 DOPED WITH 0.1 WT.% MgO
W.R. GRACE and CO.
GREEN DENSITY : 56% ρth
PARTICLE SIZE : ≈ 0.1 μm
XBL 767-7263

Figure 5.

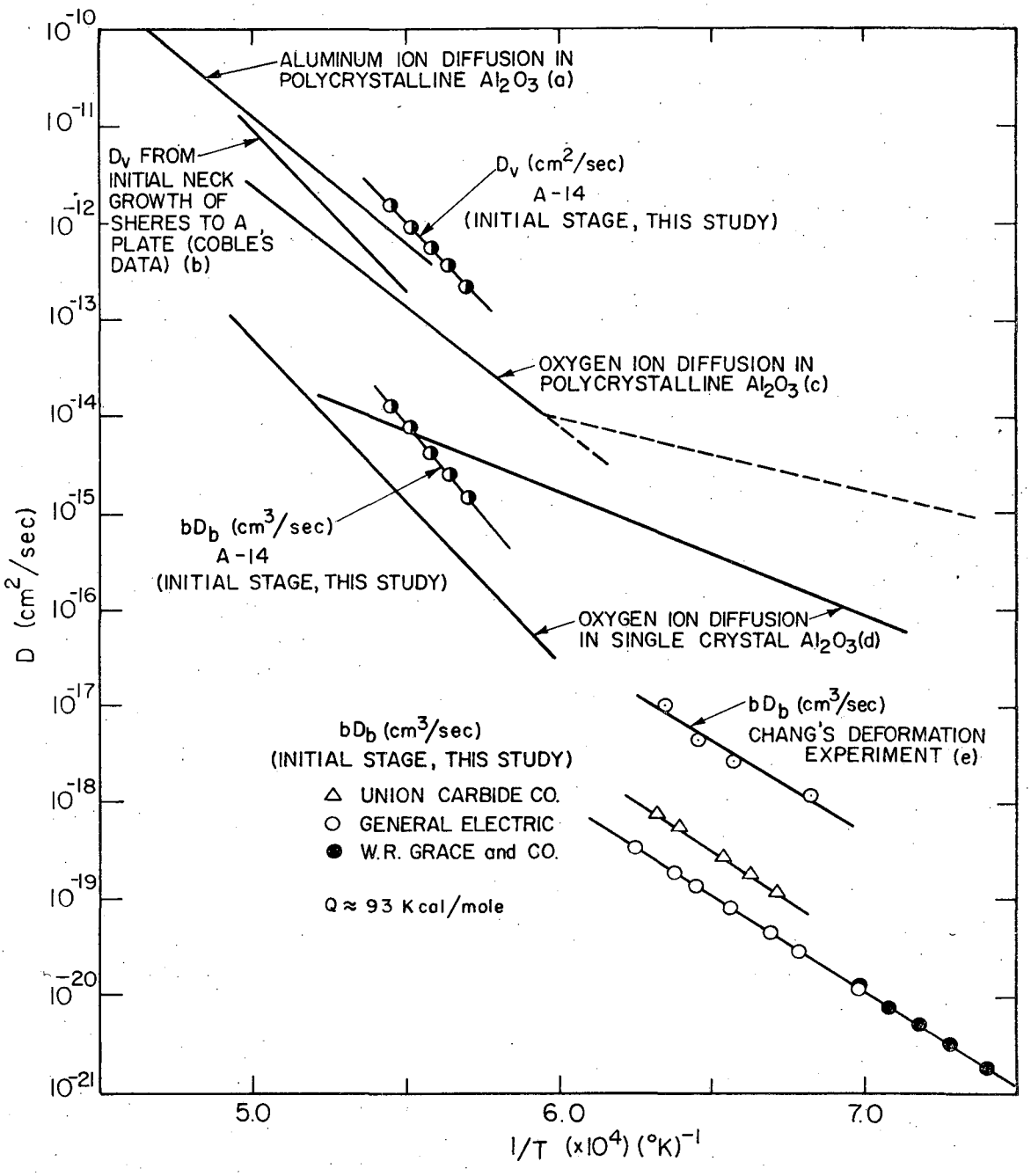
ALUMINUM ION DIFFUSION IN POLYCRYSTALLINE Al_2O_3 (a)
D_v FROM INITIAL NECK GROWTH OF SHERES TO A PLATE (COBLE'S DATA) (b)
D_v (cm^2/sec) A-14 (INITIAL STAGE, THIS STUDY)
OXYGEN ION DIFFUSION IN POLYCRYSTALLINE Al_2O_3 (c)
bD_b (cm^3/sec) A-14 (INITIAL STAGE, THIS STUDY)
OXYGEN ION DIFFUSION IN SINGLE CRYSTAL Al_2O_3(d)
bD_b (cm^3/sec) CHANG'S DEFORMATION EXPERIMENT (e)
bD_b (cm^3/sec) (INITIAL STAGE, THIS STUDY)
△ UNION CARBIDE CO.
○ GENERAL ELECTRIC
● W.R. GRACE and CO.
Q ≈ 93 Kcal/mole
D (cm^2/sec)
10^{-10}
10^{-11}
10^{-12}
10^{-13}
10^{-14}
10^{-15}
10^{-16}
10^{-17}
10^{-18}
10^{-19}
10^{-20}
10^{-21}
5.0
6.0
7.0
1/T (x10^4) ($°K$)$^{-1}$
XBL 767-7264 A

Figure 6.

TECHNICAL INFORMATION DIVISION
LAWRENCE BERKELEY LABORATORY
UNIVERSITY OF CALIFORNIA
BERKELEY, CALIFORNIA 94720